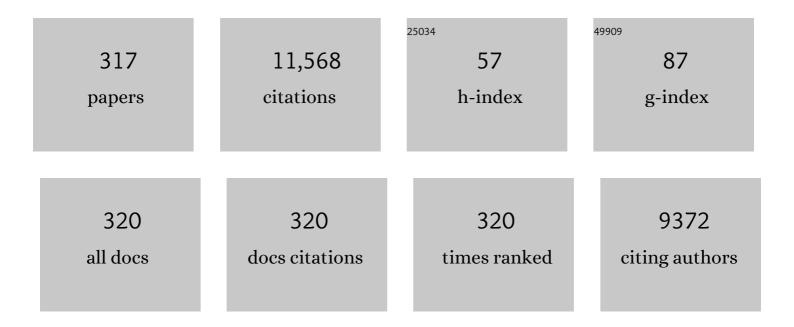
List of Publications by Year in descending order

Source: https://exaly.com/author-pdf/1412988/publications.pdf Version: 2024-02-01



MYEONG-UN KIM

#	Article	IF	CITATIONS
1	High-resolution MR imaging for nodal staging in rectal cancer: are there any criteria in addition to the size?. European Journal of Radiology, 2004, 52, 78-83.	2.6	382
2	Varying Appearances of Cholangiocarcinoma: Radiologic-Pathologic Correlation. Radiographics, 2009, 29, 683-700.	3.3	376
3	Added Value of Gadoxetic Acid–enhanced Hepatobiliary Phase MR Imaging in the Diagnosis of Hepatocellular Carcinoma. Radiology, 2010, 255, 459-466.	7.3	305
4	Differential Diagnosis of Periampullary Carcinomas at MR Imaging. Radiographics, 2002, 22, 1335-1352.	3.3	198
5	CT and PET in Stomach Cancer: Preoperative Staging and Monitoring of Response to Therapy. Radiographics, 2006, 26, 143-156.	3.3	169
6	Solid Pseudopapillary Tumor of the Pancreas: Typical and Atypical Manifestations. American Journal of Roentgenology, 2006, 187, W178-W186.	2.2	158
7	Can microvessel invasion of hepatocellular carcinoma be predicted by pre-operative MRI?. European Radiology, 2009, 19, 1744-1751.	4.5	158
8	Single Hepatocellular Carcinoma: Preoperative MR Imaging to Predict Early Recurrence after Curative Resection. Radiology, 2015, 276, 433-443.	7.3	154
9	Complete response at first chemoembolization is still the most robust predictor for favorable outcome in hepatocellular carcinoma. Journal of Hepatology, 2015, 62, 1304-1310.	3.7	148
10	Prediction of microvascular invasion of hepatocellular carcinoma: Usefulness of peritumoral hypointensity seen on gadoxetate disodiumâ€enhanced hepatobiliary phase images. Journal of Magnetic Resonance Imaging, 2012, 35, 629-634.	3.4	147
11	Biliary Dilatation: Differentiation of Benign from Malignant Causes—Value of Adding Conventional MR Imaging to MR Cholangiopancreatography. Radiology, 2000, 214, 173-181.	7.3	137
12	Preoperative Staging of Rectal Cancer With MRI: Accuracy and Clinical Usefulness. Annals of Surgical Oncology, 2000, 7, 732-737.	1.5	136
13	Perfusion CT: Noninvasive Surrogate Marker for Stratification of Pancreatic Cancer Response to Concurrent Chemo- and Radiation Therapy. Radiology, 2009, 250, 110-117.	7.3	134
14	Radiomics on Gadoxetic Acid–Enhanced Magnetic Resonance Imaging for Prediction of Postoperative Early and Late Recurrence of Single Hepatocellular Carcinoma. Clinical Cancer Research, 2019, 25, 3847-3855.	7.0	134
15	Nodular hepatocellular carcinomas: detection with arterial-, portal-, and delayed-phase images at spiral CT Radiology, 1997, 202, 383-388.	7.3	132
16	Greater and Lesser Omenta: Normal Anatomy and Pathologic Processes. Radiographics, 2007, 27, 707-720.	3.3	124
17	Imaging liver metastases: Review and update. European Journal of Radiology, 2006, 58, 217-228.	2.6	121
18	MRI-detected extramural vascular invasion is an independent prognostic factor for synchronous metastasis in patients with rectal cancer. European Radiology, 2015, 25, 1347-1355.	4.5	119

#	Article	IF	CITATIONS
19	Typical and Atypical Manifestations of Serous Cystadenoma of the Pancreas: Imaging Findings With Pathologic Correlation. American Journal of Roentgenology, 2009, 193, 136-142.	2.2	107
20	Intraabdominal Complications Secondary to Ventriculoperitoneal Shunts: CT Findings and Review of the Literature. American Journal of Roentgenology, 2009, 193, 1311-1317.	2.2	106
21	Hilar Cholangiocarcinoma: Role of Preoperative Imaging with Sonography, MDCT, MRI, and Direct Cholangiography. American Journal of Roentgenology, 2008, 191, 1448-1457.	2.2	103
22	Restaging of Rectal Cancer with MR Imaging after Concurrent Chemotherapy and Radiation Therapy. Radiographics, 2010, 30, 503-516.	3.3	103
23	Relative accuracy of CT and MRI in the differentiation of benign from malignant pancreatic cystic lesions. Clinical Radiology, 2011, 66, 315-321.	1.1	99
24	Acute cholecystitis: comparison of MR cholangiography and US Radiology, 1998, 209, 781-785.	7.3	98
25	Accuracy of gadoxetic acid-enhanced magnetic resonance imaging for the diagnosis of sinusoidal obstruction syndrome in patients with chemotherapy-treated colorectal liver metastases. European Radiology, 2012, 22, 864-871.	4.5	97
26	Sonographic findings in tuberculous epididymitis and epididymo-orchitis. , 1997, 25, 390-394.		96
27	Diffusion-weighted MR imaging of liver on 3.0-Tesla system: effect of intravenous administration of gadoxetic acid disodium. European Radiology, 2010, 20, 1052-1060.	4.5	95
28	Comparison of CT and 18F-FDG PET for Detecting Peritoneal Metastasis on the Preoperative Evaluation for Gastric Carcinoma. Korean Journal of Radiology, 2006, 7, 249.	3.4	89
29	Indicative findings of pancreatic cancer in prediagnostic CT. European Radiology, 2009, 19, 2448-2455.	4.5	88
30	Preoperative prediction of the microvascular invasion of hepatocellular carcinoma with diffusion-weighted imaging. Liver Transplantation, 2012, 18, 1171-1178.	2.4	86
31	Metal Artifact Reduction Software Used With Abdominopelvic Dual-Energy CT of Patients With Metal Hip Prostheses: Assessment of Image Quality and Clinical Feasibility. American Journal of Roentgenology, 2014, 203, 788-795.	2.2	85
32	Autologous Bone Marrow Infusion Activates the Progenitor Cell Compartment in Patients with Advanced Liver Cirrhosis. Cell Transplantation, 2010, 19, 1237-1246.	2.5	84
33	Gadoxetate Disodium-Enhanced Magnetic Resonance Imaging Versus Contrast-Enhanced 18F-Fluorodeoxyglucose Positron Emission Tomography/Computed Tomography for the Detection of Colorectal Liver Metastases. Investigative Radiology, 2011, 46, 548-555.	6.2	83
34	Perfusion MRI for the prediction of treatment response after preoperative chemoradiotherapy in locally advanced rectal cancer. European Radiology, 2012, 22, 1693-1700.	4.5	83
35	Comparison of MRI and Endoscopic Ultrasound in the Characterization of Pancreatic Cystic Lesions. American Journal of Roentgenology, 2010, 195, 947-952.	2.2	82
36	Hepatocellular Carcinoma versus Other Hepatic Malignancy in Cirrhosis: Performance of LI-RADS Version 2018. Radiology, 2019, 291, 72-80.	7.3	82

#	Article	IF	CITATIONS
37	Factors Influencing Pathologic Results after Total Mesorectal Excision for Rectal Cancer: Analysis of Consecutive 100 Cases. Annals of Surgical Oncology, 2008, 15, 721-728.	1.5	79
38	Colonic Pseudoobstruction: CT Findings. American Journal of Roentgenology, 2008, 190, 1521-1526.	2.2	79
39	Rectal Cancer: Comparison of Accuracy of Local-Regional Staging with Two- and Three-dimensional Preoperative 3-T MR Imaging. Radiology, 2010, 254, 485-492.	7.3	79
40	Comparison of gadoxetic acidâ€enhanced dynamic imaging and diffusionâ€weighted imaging for the preoperative evaluation of colorectal liver metastases. Journal of Magnetic Resonance Imaging, 2011, 34, 345-353.	3.4	79
41	Response Evaluation in Patients With Colorectal Liver Metastases: RECIST Version 1.1 Versus Modified CT Criteria. American Journal of Roentgenology, 2012, 199, 809-815.	2.2	77
42	Body Size Indexes for Optimizing lodine Dose for Aortic and Hepatic Enhancement at Multidetector CT: Comparison of Total Body Weight, Lean Body Weight, and Blood Volume. Radiology, 2010, 254, 163-169.	7.3	76
43	Focal Hepatic Lesions: Detection and Characterization with Combination Gadolinium- and Superparamagnetic Iron Oxide–enhanced MR Imaging. Radiology, 2003, 228, 719-726.	7.3	75
44	Effects of Neoadjuvant Combined Chemotherapy and Radiation Therapy on the CT Evaluation of Resectability and Staging in Patients with Pancreatic Head Cancer. Radiology, 2009, 250, 758-765.	7.3	73
45	Differentiation of Hepatic Hyperintense Lesions Seen on Gadoxetic Acid–Enhanced Hepatobiliary Phase MRI. American Journal of Roentgenology, 2011, 197, W44-W52.	2.2	72
46	Prospective comparison of prognostic values of modified Response Evaluation Criteria in Solid Tumours with European Association for the Study of the Liver criteria in hepatocellular carcinoma following chemoembolisation. European Journal of Cancer, 2013, 49, 826-834.	2.8	71
47	Growth rate of early-stage hepatocellular carcinoma in patients with chronic liver disease. Clinical and Molecular Hepatology, 2015, 21, 279.	8.9	70
48	Diagnostic accuracy of prospective application of the Liver Imaging Reporting and Data System (LI-RADS) in gadoxetate-enhanced MRI. European Radiology, 2018, 28, 2038-2046.	4.5	67
49	Accuracy in Differentiation of Mucinous and Nonmucinous Rectal Carcinoma on MR Imaging. Journal of Computer Assisted Tomography, 2003, 27, 48-55.	0.9	66
50	The Utility of F-18 FDG PET/CT in the Evaluation of Pancreatic Intraductal Papillary Mucinous Neoplasm. Clinical Nuclear Medicine, 2010, 35, 776-779.	1.3	66
51	Hepatocellular Carcinoma with Irregular Rim-Like Arterial Phase Hyperenhancement: More Aggressive Pathologic Features. Liver Cancer, 2019, 8, 24-40.	7.7	66
52	Recurrent Pyogenic Cholangitis: Comparison between MR Cholangiography and Direct Cholangiography. Radiology, 2001, 220, 677-682.	7.3	65
53	The Differential Imaging Features of Fat-Containing Tumors in the Peritoneal Cavity and Retroperitoneum: the Radiologic-Pathologic Correlation. Korean Journal of Radiology, 2010, 11, 333.	3.4	64
54	Differentiation of early hepatocellular carcinoma from benign hepatocellular nodules on gadoxetic acid-enhanced MRI. British Journal of Radiology, 2012, 85, e837-e844.	2.2	63

#	Article	IF	CITATIONS
55	Gadoxetic acid-enhanced MRI of macrotrabecular-massive hepatocellular carcinoma and its prognostic implications. Journal of Hepatology, 2021, 74, 109-121.	3.7	63
56	Hyperintense HCC on hepatobiliary phase images of gadoxetic acid-enhanced MRI: Correlation with clinical and pathological features. European Journal of Radiology, 2012, 81, 3877-3882.	2.6	62
57	Gadoxetate Disodium–Enhanced MRI of Mass-Forming Intrahepatic Cholangiocarcinomas: Imaging-Histologic Correlation. American Journal of Roentgenology, 2013, 201, W603-W611.	2.2	62
58	Comparison of diffusionâ€weighted MRI and MR volumetry in the evaluation of early treatment outcomes after preoperative chemoradiotherapy for locally advanced rectal cancer. Journal of Magnetic Resonance Imaging, 2011, 34, 570-576.	3.4	60
59	Hepatocellular carcinoma in patients with chronic liver disease: A comparison of gadoxetic acid-enhanced MRI and multiphasic MDCT. Clinical Radiology, 2012, 67, 148-156.	1.1	60
60	Comparison of breathhold, navigator-triggered, and free-breathing diffusion-weighted MRI for focal hepatic lesions. Journal of Magnetic Resonance Imaging, 2013, 38, 109-118.	3.4	58
61	Consensus Report of the 4th International Forum for Gadolinium-Ethoxybenzyl-Diethylenetriamine Pentaacetic Acid Magnetic Resonance Imaging. Korean Journal of Radiology, 2011, 12, 403.	3.4	57
62	Staging of extrahepatic cholangiocarcinoma. European Radiology, 2008, 18, 2182-2195.	4.5	56
63	Dysplastic nodules of the liver: imaging findings. Abdominal Imaging, 1999, 24, 250-257.	2.0	55
64	Curative Resection of Single Primary Hepatic Malignancy: Liver Imaging Reporting and Data System Category LR-M Portends a Worse Prognosis. American Journal of Roentgenology, 2017, 209, 576-583.	2.2	55
65	Consensus report from the 8th International Forum for Liver Magnetic Resonance Imaging. European Radiology, 2020, 30, 370-382.	4.5	55
66	Ultrasonography, Computed Tomography and Magnetic Resonance Imaging of Hepatocellular Carcinoma: Toward Improved Treatment Decisions. Oncology, 2011, 81, 86-99.	1.9	54
67	Gadoxetate Disodium–Enhanced Hepatobiliary Phase MRI of Hepatocellular Carcinoma: Correlation With Histological Characteristics. American Journal of Roentgenology, 2011, 197, 399-405.	2.2	54
68	Prediction of the histopathological grade of hepatocellular carcinoma using qualitative diffusion-weighted, dynamic, and hepatobiliary phase MRI. European Radiology, 2012, 22, 1701-1708.	4.5	54
69	Differentiation of Benign and Malignant Solid Pseudopapillary Neoplasms of the Pancreas. Journal of Computer Assisted Tomography, 2009, 33, 689-694.	0.9	53
70	Quantitative evaluation of liver cirrhosis using T1 relaxation time with 3 tesla MRI before and after oxygen inhalation. Journal of Magnetic Resonance Imaging, 2012, 36, 405-410.	3.4	52
71	Abdominal Applications of 3.0-T MR Imaging: Comparative Review versus a 1.5-T System. Radiographics, 2008, 28, e30-e30.	3.3	50
72	Liver imaging reporting and data system (LI-RADS) version 2014: understanding and application of the diagnostic algorithm. Clinical and Molecular Hepatology, 2016, 22, 296-307.	8.9	49

#	Article	IF	CITATIONS
73	MR Cholangiography in Symptomatic Gallstones: Diagnostic Accuracy according to Clinical Risk Group. Radiology, 2002, 224, 410-416.	7.3	48
74	Biliary Ductal Involvement of Hilar Cholangiocarcinoma. Journal of Computer Assisted Tomography, 2007, 31, 72-78.	0.9	48
75	Radiological and Clinical Features of Sarcomatoid Hepatocellular Carcinoma in 11 Cases. Journal of Computer Assisted Tomography, 2008, 32, 745-749.	0.9	47
76	Evaluation of treatment response in hepatocellular carcinoma in the explanted liver with Liver Imaging Reporting and Data System version 2017. European Radiology, 2020, 30, 261-271.	4.5	47
77	Early Biliary Complications of Laparoscopic Cholecystectomy:Evaluation on T2-Weighted MR Cholangiography in Conjunction with Mangafodipir Trisodium-Enhanced T1-Weighted MR Cholangiography. American Journal of Roentgenology, 2004, 183, 1559-1566.	2.2	46
78	Factors Related to Preoperative Assessment of the Circumferential Resection Margin and the Extent of Mesorectal Invasion by Magnetic Resonance Imaging in Rectal Cancer: A Prospective Comparison Study. World Journal of Surgery, 2009, 33, 1952-1960.	1.6	45
79	Hepatocarcinogenesis: imaging-pathologic correlation. Abdominal Imaging, 2011, 36, 232-243.	2.0	45
80	Hepatocellular Carcinoma Variants: Radiologic-Pathologic Correlation. American Journal of Roentgenology, 2009, 193, W7-W13.	2.2	44
81	How to utilize LR-M features of the LI-RADS to improve the diagnosis of combined hepatocellular-cholangiocarcinoma on gadoxetate-enhanced MRI?. European Radiology, 2019, 29, 2408-2416.	4.5	44
82	Comparison of LI-RADS 2018 and KLCA-NCC 2018 for noninvasive diagnosis of hepatocellular carcinoma using magnetic resonance imaging. Clinical and Molecular Hepatology, 2020, 26, 340-351.	8.9	44
83	Preoperative MRI of Rectal Cancer With and Without Rectal Water Filling:An Intraindividual Comparison. American Journal of Roentgenology, 2004, 182, 1469-1476.	2.2	43
84	Optimal Scan Window for Detection of Hypervascular Hepatocellular Carcinomas During MDCT Examination. American Journal of Roentgenology, 2006, 187, 198-206.	2.2	43
85	Liver fibrosis: stretched exponential model outperforms mono-exponential and bi-exponential models of diffusion-weighted MRI. European Radiology, 2018, 28, 2812-2822.	4.5	43
86	Gadoxetic acid–enhanced MRI as a predictor of recurrence of HCC after liver transplantation. European Radiology, 2020, 30, 987-995.	4.5	43
87	Gadoxetic acidâ€enhanced MRI findings of early hepatocellular carcinoma as defined by new histologic criteria. Journal of Magnetic Resonance Imaging, 2012, 35, 393-398.	3.4	42
88	Added value of subtraction imaging in detecting arterial enhancement in small (<3Âcm) hepatic nodules on dynamic contrast-enhanced MRI in patients at high risk of hepatocellular carcinoma. European Radiology, 2013, 23, 924-930.	4.5	42
89	Diagnosis of Hepatocellular Carcinoma with Gadoxetic Acid-Enhanced MRI: 2016 Consensus Recommendations of the Korean Society of Abdominal Radiology. Korean Journal of Radiology, 2017, 18, 427.	3.4	42
90	Gastric True Leiomyoma. Journal of Computer Assisted Tomography, 2007, 31, 204-208.	0.9	41

#	Article	IF	CITATIONS
91	Imaging features of small hepatocellular carcinomas with microvascular invasion on gadoxetic acid-enhanced MR imaging. European Journal of Radiology, 2012, 81, 2507-2512.	2.6	41
92	Added value of smooth hypointense rim in the hepatobiliary phase of gadoxetic acid-enhanced MRI in identifying tumour capsule and diagnosing hepatocellular carcinoma. European Radiology, 2017, 27, 2610-2618.	4.5	41
93	CT Diagnosis of Fitz-Hugh and Curtis Syndrome: Value of the Arterial Phase Scan. Korean Journal of Radiology, 2007, 8, 40.	3.4	40
94	Hepatic cavernous hemangioma: sonographic patterns and speed of contrast enhancement on multiphase dynamic MR imaging American Journal of Roentgenology, 1998, 171, 1021-1025.	2.2	38
95	Number of Target Lesions for EASL and Modified RECIST to Predict Survivals in Hepatocellular Carcinoma Treated with Chemoembolization. Clinical Cancer Research, 2013, 19, 1503-1511.	7.0	38
96	Feasibility of 3D navigatorâ€ŧriggered magnetic resonance cholangiopancreatography with combined parallel imaging and compressed sensing reconstruction at 3T. Journal of Magnetic Resonance Imaging, 2017, 46, 1289-1297.	3.4	38
97	Abdominal tuberculous lymphadenopathy: MR imaging findings. Abdominal Imaging, 2000, 25, 627-632.	2.0	37
98	Radiographic Findings of Primary B-Cell Lymphoma of the Stomach: Low-Grade Versus High-Grade Malignancy in Relation to the Mucosa-Associated Lymphoid Tissue Concept. American Journal of Roentgenology, 2002, 179, 1297-1304.	2.2	37
99	Characterization of focal hepatic lesions with ferumoxides-enhanced MR imaging: Utility of T1-weighted spoiled gradient recalled echo images using different echo times. Journal of Magnetic Resonance Imaging, 2002, 15, 573-583.	3.4	37
100	Diagnostic Performance of CT/MRI Liver Imaging Reporting and Data System v2017 for Hepatocellular Carcinoma: A Systematic Review and Metaâ€Analysis. Liver International, 2020, 40, 1488-1497.	3.9	37
101	Focal eosinophilic infiltration of the liver: a mimick of hepatic metastasis. Abdominal Imaging, 1999, 24, 369-372.	2.0	36
102	Radiologic findings of Mirizzi syndrome with emphasis on MRI. Yonsei Medical Journal, 2000, 41, 144.	2.2	36
103	<scp>MRI</scp> features of hepatocellular carcinoma expressing progenitor cell markers. Liver International, 2012, 32, 430-440.	3.9	36
104	Detection of liver metastases using gadoxeticâ€enhanced dynamic and 10―and 20â€minute delayed phase MR imaging. Journal of Magnetic Resonance Imaging, 2012, 35, 635-643.	3.4	36
105	Intrahepatic mass-forming cholangiocarcinoma: prognostic value of preoperative gadoxetic acid-enhanced MRI. European Radiology, 2016, 26, 407-416.	4.5	36
106	Comparison of two different injection rates of gadoxetic acid for arterial phase MRI of the liver. Journal of Magnetic Resonance Imaging, 2010, 31, 365-372.	3.4	35
107	CT-based abdominal aortic calcification score as a surrogate marker for predicting the presence of asymptomatic coronary artery disease. European Radiology, 2014, 24, 2491-2498.	4.5	35
108	Characterization of Incidental Liver Lesions: Comparison of Multidetector CT versus Gd-EOB-DTPA-Enhanced MR Imaging. PLoS ONE, 2013, 8, e66141.	2.5	34

#	Article	IF	CITATIONS
109	Mucinous versus Nonmucinous Gastric Carcinoma: Differentiation with Helical CT. Radiology, 2002, 223, 540-546.	7.3	33
110	Gallbladder lymphangioma: MR findings. Abdominal Imaging, 2002, 27, 54-57.	2.0	33
111	MR Cholangiography for Evaluation of Hilar Branching Anatomy in Transplantation of the Right Hepatic Lobe from a Living Donor. American Journal of Roentgenology, 2008, 191, 537-545.	2.2	33
112	Compressed Sensing and Parallel Imaging for Double Hepatic Arterial Phase Acquisition in Gadoxetate-Enhanced Dynamic Liver Magnetic Resonance Imaging. Investigative Radiology, 2019, 54, 374-382.	6.2	33
113	Retrospective comparison of EASL 2018 and LI-RADS 2018 for the noninvasive diagnosis of hepatocellular carcinoma using magnetic resonance imaging. Hepatology International, 2020, 14, 70-79.	4.2	33
114	Current Limitations and Potential Breakthroughs for the Early Diagnosis of Hepatocellular Carcinoma. Gut and Liver, 2011, 5, 15-21.	2.9	33
115	Preoperative MRI of Potential Living-Donor-Related Liver Transplantation Using a Single Dose of Gadobenate Dimeglumine. American Journal of Roentgenology, 2005, 185, 424-431.	2.2	32
116	Differentiation of Adrenal Adenoma and Nonadenoma in Unenhanced CT: New Optimal Threshold Value and the Usefulness of Size Criteria for Differentiation. Korean Journal of Radiology, 2007, 8, 328.	3.4	32
117	Pancreatic Tumors: Emphasis on CT Findings and Pathologic Classification. Korean Journal of Radiology, 2011, 12, 731.	3.4	32
118	Cost evaluation of gadoxetic acid-enhanced magnetic resonance imaging in the diagnosis of colorectal-cancer metastasis in the liver: Results from the VALUE Trial. European Radiology, 2016, 26, 4121-4130.	4.5	32
119	Rectal Mucinous Adenocarcinoma: MR Imaging Assessment of Response to Concurrent Chemotherapy and Radiation Therapy—A Hypothesis-generating Study. Radiology, 2017, 285, 124-133.	7.3	32
120	CT/MRI and CEUS LI-RADS Major Features Association with Hepatocellular Carcinoma: Individual Patient Data Meta-Analysis. Radiology, 2022, 302, 326-335.	7.3	32
121	Detection and characterization of focal hepatic lesions: Mangafodipir vs. Superparamagnetic iron oxide-enhanced magnetic resonance imaging. Journal of Magnetic Resonance Imaging, 2004, 20, 612-621.	3.4	31
122	Differential Features of Pancreatobiliary- and Intestinal-type Ampullary Carcinomas at MR Imaging. Radiology, 2010, 257, 384-393.	7.3	31
123	Differentiation of benign and malignant ampullary obstructions on MR imaging. European Journal of Radiology, 2011, 80, 198-203.	2.6	31
124	Radiation Dose Reduction via Sinogram Affirmed Iterative Reconstruction and Automatic Tube Voltage Modulation (CARE kV) in Abdominal CT. Korean Journal of Radiology, 2013, 14, 886.	3.4	31
125	Perfusion Parameters of Dynamic Contrast-Enhanced Magnetic Resonance Imaging in Patients with Rectal Cancer: Correlation with Microvascular Density and Vascular Endothelial Growth Factor Expression. Korean Journal of Radiology, 2013, 14, 878.	3.4	31
126	Noncontrast magnetic resonance imaging versus ultrasonography for hepatocellular carcinoma surveillance (MIRACLE-HCC): study protocol for a prospective randomized trial. BMC Cancer, 2018, 18, 915.	2.6	31

#	Article	IF	CITATIONS
127	Tailgut Cyst: Multilocular Cystic Appearance on MRI. Journal of Computer Assisted Tomography, 1997, 21, 731.	0.9	31
128	Dynamic enhancement pattern of <scp>HCC</scp> smaller than 3Âcm in diameter on gadoxetic acidâ€enhanced <scp>MRI</scp> : comparison with multiphasic <scp>MDCT</scp> . Liver International, 2014, 34, 1593-1602.	3.9	30
129	Dedifferentiated liposarcoma of retroperitoneum: spectrum of imaging findings in 15 patients. Clinical Imaging, 2010, 34, 203-210.	1.5	29
130	Prediction of Postoperative Pancreatic Fistulas After Pancreatectomy. Journal of Ultrasound in Medicine, 2014, 33, 781-786.	1.7	28
131	Gadoxetic acid-enhanced magnetic resonance imaging: Hepatocellular carcinoma and mimickers. Clinical and Molecular Hepatology, 2019, 25, 223-233.	8.9	28
132	Advanced Gastric Carcinoma With Signet Ring Cell Carcinoma Versus Non-Signet Ring Cell Carcinoma. Journal of Computer Assisted Tomography, 2006, 30, 880-884.	0.9	27
133	A case of mesenteric cystic lymphangioma: Fat saturation and chemical shift MR imaging. Journal of Magnetic Resonance Imaging, 2006, 23, 77-80.	3.4	27
134	Single breathâ€hold multiarterial dynamic MRI of the liver at 3T using a 3D fatâ€suppressed keyhole technique. Journal of Magnetic Resonance Imaging, 2008, 28, 396-402.	3.4	27
135	Intraductal ultrasonography combined with percutaneous transhepatic cholangioscopy for the preoperative evaluation of longitudinal tumor extent in hilar cholangiocarcinoma. Journal of Gastroenterology and Hepatology (Australia), 2010, 25, 286-292.	2.8	27
136	Histological characteristics of small hepatocellular carcinomas showing atypical enhancement patterns on gadoxetic acidâ€enhanced MR imaging. Journal of Magnetic Resonance Imaging, 2013, 37, 1384-1391.	3.4	27
137	Imaging features related with prognosis of hepatocellular carcinoma. Abdominal Radiology, 2019, 44, 509-516.	2.1	27
138	A proposal of imaging classification of intrahepatic mass-forming cholangiocarcinoma into ductal and parenchymal types: clinicopathologic significance. European Radiology, 2019, 29, 3111-3121.	4.5	27
139	Preoperative Staging Accuracy of Multidetector Row Computed Tomography for Extrahepatic Bile Duct Carcinoma. Journal of Computer Assisted Tomography, 2006, 30, 362-367.	0.9	26
140	Intraindividual Comparison of Diagnostic Performance in Patients With Hepatic Metastasis of Full-Dose Standard and Half-Dose Iterative Reconstructions With Dual-Source Abdominal Computed Tomography. Investigative Radiology, 2014, 49, 195-200.	6.2	26
141	Percutaneous Sclerotherapy of Renal Cysts with a Beta-Emitting Radionuclide, Holmium-166-chitosan Complex. Korean Journal of Radiology, 2004, 5, 128.	3.4	25
142	Choledochal Cyst and Anomalous Pancreaticobiliary Ductal Union in Adults. Journal of Computer Assisted Tomography, 2008, 32, 17-22.	0.9	25
143	Role of EUS and MDCT in the diagnosis of gastric submucosal tumors according to the revised pathologic concept of gastrointestinal stromal tumors. European Radiology, 2009, 19, 924-934.	4.5	25
144	Histogram Analysis of Gadoxetic Acid-Enhanced MRI for Quantitative Hepatic Fibrosis Measurement. PLoS ONE, 2014, 9, e114224.	2.5	25

#	Article	IF	CITATIONS
145	Comparison of the use of the transrectal surface coil and the pelvic phased-array coil in MR imaging for preoperative evaluation of uterine cervical carcinoma American Journal of Roentgenology, 1997, 168, 1215-1221.	2.2	24
146	Magnetic resonance cholangiography: comparison of two- and three-dimensional sequences for assessment of malignant biliary obstruction. European Radiology, 2008, 18, 78-86.	4.5	24
147	Detection of hepatic hypovascular metastases: 3D gradient echo MRI using a hepatobiliary contrast agent. Journal of Magnetic Resonance Imaging, 2010, 31, 571-578.	3.4	24
148	MRI Findings of Rectal Submucosal Tumors. Korean Journal of Radiology, 2011, 12, 487.	3.4	24
149	Quantitative Analysis of the Effect of Iterative Reconstruction Using a Phantom: Determining the Appropriate Blending Percentage. Yonsei Medical Journal, 2015, 56, 253.	2.2	24
150	Preoperative Radiologic and Postoperative Pathologic Risk Factors for Early Intra-Hepatic Recurrence in Hepatocellular Carcinoma Patients Who Underwent Curative Resection. Yonsei Medical Journal, 2009, 50, 789.	2.2	23
151	Detection of recurrent hepatocellular carcinoma on post-operative surveillance: comparison of MDCT and gadoxetic acid-enhanced MRI. Abdominal Imaging, 2014, 39, 291-299.	2.0	23
152	Pitfalls and problems to be solved in the diagnostic CT/MRI Liver Imaging Reporting and Data System (LI-RADS). European Radiology, 2019, 29, 1124-1132.	4.5	23
153	Hepatic sarcomatoid carcinoma: magnetic resonance imaging evaluation by using the liver imaging reporting and data system. European Radiology, 2019, 29, 3761-3771.	4.5	23
154	Using Kinematic MR Cholangiopancreatography to Evaluate Biliary Dilatation. American Journal of Roentgenology, 2002, 178, 909-914.	2.2	22
155	Fat Sparing of Surrounding Liver From Metastasis in Patients with Fatty Liver: MR Imaging with Histopathologic Correlation. American Journal of Roentgenology, 2003, 180, 1347-1350.	2.2	22
156	Prognostic role of magnetic resonance imaging vs. computed tomography for hepatocellular carcinoma undergoing chemoembolization. Liver International, 2015, 35, 1722-1730.	3.9	22
157	T2-weighted signal intensity-selected volumetry for prediction of pathological complete response after preoperative chemoradiotherapy in locally advanced rectal cancer. European Radiology, 2018, 28, 5231-5240.	4.5	22
158	Characterization of focal liver lesions using the stretched exponential model: comparison with monoexponential and biexponential diffusion-weighted magnetic resonance imaging. European Radiology, 2019, 29, 5111-5120.	4.5	22
159	Intraindividual Comparison between Gadoxetate-Enhanced Magnetic Resonance Imaging and Dynamic Computed Tomography for Characterizing Focal Hepatic Lesions: A Multicenter, Multireader Study. Korean Journal of Radiology, 2019, 20, 1616.	3.4	22
160	Intraductal papillary neoplasm of the bile duct: Assessment of invasive carcinoma and long-term outcomes using MRI. Journal of Hepatology, 2019, 70, 692-699.	3.7	22
161	Colorectal Mucinous Carcinoma: Findings on MRI. Journal of Computer Assisted Tomography, 1999, 23, 291-296.	0.9	22
162	Possible Contrast Media Reduction with Low keV Monoenergetic Images in the Detection of Focal Liver Lesions: A Dual-Energy CT Animal Study. PLoS ONE, 2015, 10, e0133170.	2.5	21

#	Article	IF	CITATIONS
163	Acute thrombosis of a portal vein aneurysm and development. Clinical Radiology, 2004, 59, 631-633.	1.1	20
164	Unusual Cystic Neoplasms in the Pancreas. Journal of Computer Assisted Tomography, 2005, 29, 610-616.	0.9	20
165	Detection of hepatic metastasis: Manganese- and ferucarbotran-enhanced MR imaging. European Journal of Radiology, 2006, 60, 84-90.	2.6	20
166	Mangafodipir trisodium-enhanced MRI for the detection and characterization of focal hepatic lesions: Is delayed imaging useful?. Journal of Magnetic Resonance Imaging, 2006, 23, 706-711.	3.4	20
167	Magnetic Resonance Imaging of Hepatocellular Carcinoma Using Contrast Media. Oncology, 2008, 75, 72-82.	1.9	20
168	18F-FDG PET Metabolic Parameters and MRI Perfusion and Diffusion Parameters in Hepatocellular Carcinoma: A Preliminary Study. PLoS ONE, 2013, 8, e71571.	2.5	20
169	Imaging Findings of Liposuction with an Emphasis on Postsurgical Complications. Korean Journal of Radiology, 2015, 16, 1197.	3.4	20
170	Feasibility of mesorectal vascular invasion in predicting early distant metastasis in patients with stage T3 rectal cancer based on rectal MRI. European Radiology, 2016, 26, 297-305.	4.5	20
171	Feasibility of Simultaneous Multislice Acceleration Technique in Diffusion-Weighted Magnetic Resonance Imaging of the Rectum. Korean Journal of Radiology, 2020, 21, 77.	3.4	20
172	The Modified Response Evaluation Criteria in Solid Tumors (RECIST) Yield a More Accurate Prognoses Than the RECIST 1.1 in Hepatocellular Carcinoma Treated with Transarterial Radioembolization. Gut and Liver, 2020, 14, 765-774.	2.9	20
173	Atypical Inside-Out Pattern of Hepatic Hemangiomas. American Journal of Roentgenology, 2000, 174, 1571-1574.	2.2	19
174	Diffusion and perfusion MRI prediction of progressionâ€ f ree survival in patients with hepatocellular carcinoma treated with concurrent chemoradiotherapy. Journal of Magnetic Resonance Imaging, 2014, 39, 286-292.	3.4	19
175	Hepatic Iron Deposition on Magnetic Resonance Imaging: Correlation with Inflammatory Activity. Journal of Computer Assisted Tomography, 2002, 26, 988-993.	0.9	18
176	Mucosa-Associated Lymphoid Tissue Lymphoma of the Esophagus Coexistent with Bronchus-Associated Lymphoid Tissue Lymphoma of the Lung. Yonsei Medical Journal, 2005, 46, 562.	2.2	18
177	Preoperative Evaluation of Common Bile Duct Stones in Patients with Gallstone Disease. American Journal of Roentgenology, 2005, 184, 1854-1859.	2.2	18
178	Optimal Delay Time for the Hepatic Parenchymal Enhancement at the Multidetector CT Examination. Journal of Computer Assisted Tomography, 2006, 30, 182-188.	0.9	18
179	Optimal T2-weighted MR Cholangiopancreatographic Images Can Be Obtained after Administration of Gadoxetic Acid. Radiology, 2010, 256, 475-484.	7.3	18
180	Problematic lesions in cirrhotic liver mimicking hepatocellular carcinoma. European Radiology, 2019, 29, 5101-5110.	4.5	18

#	Article	IF	CITATIONS
181	Stratification of Postsurgical Computed Tomography Surveillance Based on the Extragastric Recurrence of Early Gastric Cancer. Annals of Surgery, 2020, 272, 319-325.	4.2	18
182	Preoperative Imaging of Sentinel Lymph Nodes in Gastric Cancer Using CT Lymphography. Yonsei Medical Journal, 2010, 51, 407.	2.2	17
183	Hyperintense Lesions on Gadoxetate Disodium-Enhanced Hepatobiliary Phase Imaging. American Journal of Roentgenology, 2012, 199, W575-W586.	2.2	17
184	Histologic Characteristics of Hepatocellular Carcinomas Showing Atypical Enhancement Patterns on 4-Phase MDCT Examination. Korean Journal of Radiology, 2012, 13, 586.	3.4	17
185	Extracellular contrast agent-enhanced MRI: 15-min delayed phase may improve the diagnostic performance for hepatocellular carcinoma in patients with chronic liver disease. European Radiology, 2018, 28, 1551-1559.	4.5	17
186	MRI Ancillary Features for LI-RADS Category 3 and 4 Observations: Improved Categorization to Indicate the Risk of Hepatic Malignancy. American Journal of Roentgenology, 2020, 215, 1354-1362.	2.2	17
187	Failure of hepatocellular carcinoma surveillance: inadequate echogenic window and macronodular parenchyma as potential culprits. Ultrasonography, 2019, 38, 311-320.	2.3	17
188	Aberrant expression of OATP1B3 in colorectal cancer liver metastases and its clinical implication on gadoxetic acid-enhanced MRI. Oncotarget, 2017, 8, 71012-71023.	1.8	17
189	Comparison of CT and MRI for presurgical characterization of paraaortic lymph nodes in patients with pancreatico-biliary carcinoma. World Journal of Gastroenterology, 2008, 14, 2208.	3.3	17
190	Paraaortic lymph node metastasis in patients with intra-abdominal malignancies: CT vs PET. World Journal of Gastroenterology, 2009, 15, 4434.	3.3	17
191	Incremental Role of Pancreatic Magnetic Resonance Imaging after Staging Computed Tomography to Evaluate Patients with Pancreatic Ductal Adenocarcinoma. Cancer Research and Treatment, 2019, 51, 24-33.	3.0	17
192	Mangafodipir trisodium-enhanced MRI of hepatocellular carcinoma: correlation with histological characteristics. Clinical Radiology, 2008, 63, 1195-1204.	1.1	16
193	Metastasis Versus Focal Eosinophilic Infiltration of the Liver in Patients With Extrahepatic Abdominal Cancer. Journal of Computer Assisted Tomography, 2009, 33, 119-124.	0.9	16
194	Management of subcentimetre arterially enhancing and hepatobiliary hypointense lesions on gadoxetic acid-enhanced MRI in patients at risk for HCC. European Radiology, 2018, 28, 1476-1484.	4.5	16
195	Imaging Features of Hepatocellular Carcinoma. Investigative Radiology, 2019, 54, 494-499.	6.2	16
196	Quantitative assessment of mesorectal fat: new prognostic biomarker in patients with mid-to-lower rectal cancer. European Radiology, 2019, 29, 1240-1247.	4.5	16
197	Application of Liver Imaging Reporting and Data System version 2018 ancillary features to upgrade from LR-4 to LR-5 on gadoxetic acid–enhanced MRI. European Radiology, 2021, 31, 855-863.	4.5	16
198	Clinical Implication of Positive Oral Contrast Computed Tomography for the Evaluation of Postoperative Leakage After Gastrectomy for Gastric Cancer. Journal of Computer Assisted Tomography, 2010, 34, 537-542.	0.9	15

#	Article	IF	CITATIONS
199	Can preoperative diffusion-weighted MRI predict postoperative hepatic insufficiency after curative resection of HBV-related hepatocellular carcinoma? A pilot study. Magnetic Resonance Imaging, 2010, 28, 802-811.	1.8	15
200	Focal Eosinophilic Infiltration of the Liver. Journal of Computer Assisted Tomography, 2011, 35, 81-85.	0.9	15
201	Distinguishing hemangiomas from malignant solid hepatic lesions: A comparison of heavily T2â€weighted images obtained before and after administration of gadoxetic acid. Journal of Magnetic Resonance Imaging, 2011, 34, 310-317.	3.4	15
202	Usefulness of the Tensile Gallbladder Fundus Sign in the Diagnosis of Early Acute Cholecystitis. American Journal of Roentgenology, 2013, 201, 340-346.	2.2	15
203	ls Non-Contrast CT Adequate for the Evaluation of Hepatic Metastasis in Patients Who Cannot Receive Iodinated Contrast Media?. PLoS ONE, 2015, 10, e0134133.	2.5	15
204	Impact of Reference Standard on CT, MRI, and Contrast-enhanced US LI-RADS Diagnosis of Hepatocellular Carcinoma: A Meta-Analysis. Radiology, 2022, 303, 544-545.	7.3	15
205	Evaluation of Biliary Malignancies Using Multidetector-Row Computed Tomography. Journal of Computer Assisted Tomography, 2010, 34, 496-505.	0.9	14
206	Using multi-detector-row CT to diagnose ampullary adenoma or adenocarcinoma in situ. European Journal of Radiology, 2011, 80, e340-e345.	2.6	14
207	Cumulative Radiation Exposure during Follow-Up after Curative Surgery for Gastric Cancer. Korean Journal of Radiology, 2012, 13, 144.	3.4	14
208	Novel Imaging Diagnosis for Hepatocellular Carcinoma: Consensus from the 5th Asia-Pacific Primary Liver Cancer Expert Meeting (APPLE 2014). Liver Cancer, 2015, 4, 215-227.	7.7	14
209	Health economic evaluation of Gd-EOB-DTPA MRI vs ECCM-MRI and multi-detector computed tomography in patients with suspected hepatocellular carcinoma in Thailand and South Korea. Journal of Medical Economics, 2016, 19, 759-768.	2.1	14
210	Lack of anti-tumor activity by anti-VEGF treatments in hepatic hemangiomas. Angiogenesis, 2016, 19, 147-153.	7.2	14
211	T1 bright appendix sign to exclude acute appendicitis in pregnant women. European Radiology, 2017, 27, 3310-3316.	4.5	14
212	Characteristics and Early Recurrence of Hepatocellular Carcinomas Categorized as <scp>LRâ€M</scp> : Comparison with Those Categorized as <scp>LR</scp> â€4 or 5. Journal of Magnetic Resonance Imaging, 2021, 54, 1446-1454.	3.4	14
213	Solitary Fibrous Tumor Arising from Stomach: CT Findings. Yonsei Medical Journal, 2007, 48, 1056.	2.2	13
214	Nonhypervascular Hypoattenuating Nodules Depicted on Either Portal or Equilibrium Phase Multiphasic CT Images in the Cirrhotic Liver. American Journal of Roentgenology, 2008, 191, 207-214.	2.2	13
215	Three-dimensional contrast-enhanced hepatic MR imaging: Comparison between a centric technique and a linear approach with partial Fourier along both slice and phase directions. Journal of Magnetic Resonance Imaging, 2011, 33, 160-166.	3.4	13
216	Assessment of Preoperative Magnetic Resonance Imaging Staging in Patients With Hepatocellular Carcinoma Undergoing Resection Compared With the Seventh American Joint Committee on Cancer System. Investigative Radiology, 2012, 47, 634-641.	6.2	13

#	Article	IF	CITATIONS
217	Cavernous hemangioma arising from the lesser omentum: MR findings. Abdominal Imaging, 2000, 25, 542-544.	2.0	12
218	Gadobenate Dimeglumine as an Intrabiliary Contrast Agent: Comparison with Mangafodipir Trisodium with Respect to Non-dilated Biliary Tree Depiction. Korean Journal of Radiology, 2005, 6, 229.	3.4	12
219	Optimal TE for SPIO-Enhanced Gradient-Recalled Echo MRI for the Detection of Focal Hepatic Lesions. American Journal of Roentgenology, 2006, 187, W255-W266.	2.2	12
220	Spontaneous Regression of a Cystic Tumor in a Postpartum Woman; Is It A Cystic Lymphangioma?. Yonsei Medical Journal, 2007, 48, 715.	2.2	12
221	Should Threshold Growth Be Considered a Major Feature in the Diagnosis of Hepatocellular Carcinoma Using LI-RADS?. Korean Journal of Radiology, 2021, 22, 1628.	3.4	12
222	Large Villous Adenoma in Rectum Mimicking Cerebral Hemispheres. American Journal of Roentgenology, 2000, 175, 1465-1466.	2.2	12
223	Assessment of the Prognostic Factors for a Local Recurrence of Rectal Cancer: the Utility of Preoperative MR Imaging. Korean Journal of Radiology, 2005, 6, 8.	3.4	11
224	Imaging-Guided Minimally Invasive Laparoscopic Resection of Intraluminal Small-Bowel Tumor: Report of Two Cases. American Journal of Roentgenology, 2007, 189, 56-60.	2.2	11
225	Comparison of diagnostic performance between single- and multiphasic contrast-enhanced abdominopelvic computed tomography in patients admitted to the emergency department with abdominal pain: potential radiation dose reduction. European Radiology, 2015, 25, 1048-1058.	4.5	11
226	Clinical Feasibility of MR Elastography in Patients With Biliary Obstruction. American Journal of Roentgenology, 2018, 210, 1273-1278.	2.2	11
227	Hepatobiliary versus Extracellular MRI Contrast Agents in Hepatocellular Carcinoma Detection: Hepatobiliary Phase Features in Relation to Disease-free Survival. Radiology, 2019, 293, 594-604.	7.3	11
228	Dynamic Contrast-Enhanced Magnetic Resonance Imaging as a Surrogate Biomarker for Bevacizumab in Colorectal Cancer Liver Metastasis: A Single-Arm, Exploratory Trial. Cancer Research and Treatment, 2016, 48, 1210-1221.	3.0	11
229	Variation of the Time to Aortic Enhancement of Fixed-Duration Versus Fixed-Rate Injection Protocols. American Journal of Roentgenology, 2006, 186, 185-192.	2.2	10
230	Development of hepatocellular carcinomas in patients with absence of tumors on a prior ultrasound examination. European Journal of Radiology, 2012, 81, 1450-1454.	2.6	10
231	Diagnostic Radiation Exposure of Injury Patients in the Emergency Department: A Cross-Sectional Large Scaled Study. PLoS ONE, 2013, 8, e84870.	2.5	10
232	MRI Risk Stratification for Tumor Relapse in Rectal Cancer Achieving Pathological Complete Remission after Neoadjuvant Chemoradiation Therapy and Curative Resection. PLoS ONE, 2016, 11, e0146235.	2.5	10
233	Feasibility of Preoperative FDG PET/CT Total Hepatic Glycolysis in the Remnant Liver for the Prediction of Postoperative Liver Function. American Journal of Roentgenology, 2017, 208, 624-631.	2.2	10
234	Comparison of multiplexed sensitivity encoding and single-shot echo-planar imaging for diffusion-weighted imaging of the liver. European Journal of Radiology, 2020, 132, 109292.	2.6	10

#	Article	IF	CITATIONS
235	Diagnostic performance of the LR-M criteria and spectrum of LI-RADS imaging features among primary hepatic carcinomas. Abdominal Radiology, 2020, 45, 3743-3754.	2.1	10
236	Diagnostic performance of Liver Imaging Reporting and Data System in patients at risk of both hepatocellular carcinoma and metastasis. Abdominal Radiology, 2020, 45, 3789-3799.	2.1	10
237	Gadoxetic acid-enhanced MRI of hepatocellular carcinoma: Diagnostic performance of category-adjusted LR-5 using modified criteria. PLoS ONE, 2020, 15, e0242344.	2.5	10
238	T2-weighted fast spin-echo MR findings of adenocarcinoma of the uterine cervix: comparison with squamous cell carcinoma. Yonsei Medical Journal, 1999, 40, 226.	2.2	9
239	Double common bile duct: Curvedâ€planar reformatted computed tomography (CT) and gadobenate dimeglumine–enhanced MR cholangiography. Journal of Magnetic Resonance Imaging, 2008, 27, 209-211.	3.4	9
240	Focal Eosinophilic Necrosis on Superparamagnetic Iron Oxide–Enhanced MRI. American Journal of Roentgenology, 2010, 194, 1296-1302.	2.2	9
241	Hepatocellular carcinoma: clinical and radiological findings in patients with chronic B viral hepatitis and chronic C viral hepatitis. Abdominal Imaging, 2012, 37, 591-594.	2.0	9
242	CT features of hepatic metastases from hepatoid adenocarcinoma. Abdominal Radiology, 2017, 42, 2402-2409.	2.1	9
243	Optimal criteria for hepatocellular carcinoma diagnosis using CT in patients undergoing liver transplantation. European Radiology, 2019, 29, 1022-1031.	4.5	9
244	Dynamic contrast-enhanced MRI coupled with a subtraction technique is useful for treatment response evaluation of malignant melanoma hepatic metastasis. Oncotarget, 2016, 7, 38513-38522.	1.8	9
245	Bowel Angioedema Associated With Iodinated Contrast Media. Investigative Radiology, 2017, 52, 514-521.	6.2	8
246	Feasibility of radiation dose reduction with iterative reconstruction in abdominopelvic CT for patients with inappropriate arm positioning. PLoS ONE, 2018, 13, e0209754.	2.5	8
247	Gadoxetic acid enhanced magnetic resonance imaging for prediction of the postoperative prognosis of intrahepatic mass-forming cholangiocarcinoma. Abdominal Radiology, 2019, 44, 110-121.	2.1	8
248	Preoperative Clinical and Computed Tomography (CT)-Based Nomogram to Predict Oncologic Outcomes in Patients with Pancreatic Head Cancer Resected with Curative Intent: A Retrospective Study. Journal of Clinical Medicine, 2019, 8, 1749.	2.4	8
249	Evaluation of Early Response to Treatment of Hepatocellular Carcinoma with Yttrium-90 Radioembolization Using Quantitative Computed Tomography Analysis. Korean Journal of Radiology, 2019, 20, 449.	3.4	8
250	FDG Uptake in PET by Bladder Hernia Simulating Inguinal Metastasis. Yonsei Medical Journal, 2007, 48, 886.	2.2	8
251	Magnetic Resonance Imaging for Colorectal Cancer Metastasis to the Liver: Comparative Effectiveness Research for the Choice of Contrast Agents. Cancer Research and Treatment, 2018, 50, 60-70.	3.0	8
252	Potential Conditions Causing Impairment of Selective Hepatobiliary Enhancement of Gadobenate Dimeglumine-Enhanced Delayed Magnetic Resonance Imaging. Journal of Computer Assisted Tomography, 2010, 34, 113-120.	0.9	7

#	Article	IF	CITATIONS
253	Quantification of superparamagnetic iron oxideâ€mediated signal intensity change in patients with liver cirrhosis using T2 and T2* mapping: A preliminary report. Journal of Magnetic Resonance Imaging, 2010, 31, 1379-1386.	3.4	7
254	A Multiloculated Cystic Mass in the Liver. Gastroenterology, 2010, 138, e1-e2.	1.3	7
255	Liver trauma diagnosis with contrast-enhanced ultrasound: interobserver variability between radiologist and emergency physician in an animal study. American Journal of Emergency Medicine, 2012, 30, 1229-1234.	1.6	7
256	Use of Preoperative MRI to Select Candidates for Local Excision of MRI-Staged T1 and T2 Rectal Cancer. Diseases of the Colon and Rectum, 2015, 58, 923-930.	1.3	7
257	Contrast-Enhanced CT with Knowledge-Based Iterative Model Reconstruction for the Evaluation of Parotid Gland Tumors: A Feasibility Study. Korean Journal of Radiology, 2018, 19, 957.	3.4	7
258	Metal implants influence CT scan parameters leading to increased local radiation exposure: A proposal for correction techniques. PLoS ONE, 2019, 14, e0221692.	2.5	7
259	Liver MRI with amide proton transfer imaging: feasibility and accuracy for the characterization of focal liver lesions. European Radiology, 2021, 31, 222-231.	4.5	7
260	Noninvasive evaluation of liver fibrosis: comparison of the stretched exponential diffusion-weighted model to other diffusion-weighted MRI models and transient elastography. European Radiology, 2021, 31, 4813-4823.	4.5	7
261	The Impact of CT Follow-Up Interval on Stages of Hepatocellular Carcinomas Detected During the Surveillance of Patients With Liver Cirrhosis. American Journal of Roentgenology, 2012, 199, 816-821.	2.2	6
262	Optimisation of the MR protocol in pregnant women with suspected acute appendicitis. European Radiology, 2018, 28, 514-521.	4.5	6
263	Gadolinium retention in rat abdominal organs after administration of gadoxetic acid disodium compared to gadodiamide and gadobutrol. Magnetic Resonance in Medicine, 2020, 84, 2124-2132.	3.0	6
264	Imaging findings of biliary and nonbiliary complications following laparoscopic surgery. European Radiology, 2006, 16, 1906-1914.	4.5	5
265	A Pancreatic Mass Presented With Multiple Hot Spots in the Subcutaneous Fat Layer on Positron Emission Tomography. Gastroenterology, 2010, 139, e10-e11.	1.3	5
266	Relationship between severity of liver dysfunction and the relative ratio of liver to aortic enhancement (RE) on MRI using hepatocyteâ€specific contrast. Journal of Magnetic Resonance Imaging, 2014, 39, 24-30.	3.4	5
267	Inter-observer variability of response evaluation criteria for hepatocellular carcinoma treated with chemoembolization. Digestive and Liver Disease, 2015, 47, 682-688.	0.9	5
268	Normal Postoperative Computed Tomography Findings after a Variety of Pancreatic Surgeries. Korean Journal of Radiology, 2017, 18, 299.	3.4	5
269	Prognostic significance of preoperative CT findings in patients with advanced gastric cancer who underwent curative gastrectomy. PLoS ONE, 2018, 13, e0202207.	2.5	5
270	Is there association between statin usage and contrast-associated acute kidney injury after intravenous administration of iodine-based contrast media in enhanced computed tomography?. European Radiology, 2020, 30, 5261-5271.	4.5	5

#	Article	IF	CITATIONS
271	Prognostic factors of gadoxetic acid–enhanced MRI for postsurgical outcomes in multicentric hepatocellular carcinoma. European Radiology, 2021, 31, 3405-3416.	4.5	5
272	Extended application of subtraction arterial phase imaging in Ll-RADS version 2018: a strategy to improve the diagnostic performance for hepatocellular carcinoma on gadoxetate disodium–enhanced MRI. European Radiology, 2021, 31, 1620-1629.	4.5	5
273	Incorporation of Ancillary MRI Features Into the LI-RADS Treatment Response Algorithm: Impact on Diagnostic Performance After Locoregional Treatment of Hepatocellular Carcinoma. American Journal of Roentgenology, 2022, 218, 484-493.	2.2	5
274	A dichotomous imaging classification for cholangiocarcinomas based on new histologic concepts. European Journal of Radiology, 2019, 113, 182-187.	2.6	4
275	Perirectal Cystic Paragonimiasis: Endorectal Coil MRI. Journal of Computer Assisted Tomography, 1999, 23, 94-95.	0.9	4
276	Follow-up Results After Negative Findings on Unenhanced Hepatic MR Imaging for Hepatic Metastasis from Rectal Cancer. Korean Journal of Radiology, 2004, 5, 225.	3.4	3
277	MR prediction of pathologic complete response and early-stage rectal cancer after neoadjuvant chemoradiation in patients with clinical T1/T2 rectal cancer for organ saving strategy. Medicine (United States), 2020, 99, e22746.	1.0	3
278	Benign focal liver lesions masquerading as primary liver cancers on MRI. Diagnostic and Interventional Radiology, 2020, 26, 168-175.	1.5	3
279	Hepatobiliary phase signal intensity: A potential method of diagnosing HCC with atypical imaging features among LR-M observations. PLoS ONE, 2021, 16, e0257308.	2.5	3
280	Improving Survival with Gadoxetic Acid–enhanced MRI for Hepatocellular Carcinoma. Radiology, 2020, 295, 125-126.	7.3	3
281	Comparison of Sensitivity Encoding (SENSE) and Compressed Sensing-SENSE for Contrast-Enhanced T1-Weighted Imaging in Patients With Crohn Disease Undergoing MR Enterography. American Journal of Roentgenology, 2021, , .	2.2	3
282	Characterisation of small hypoattenuating hepatic lesions in multi-detector CT (MDCT) in patients with underlying extrahepatic malignancy: added value of contrast-enhanced MR images. European Radiology, 2010, 20, 2853-2861.	4.5	2
283	An Insidious Pancreatic Lesion in a Young Woman With Recurrent Pancreatitis. Gastroenterology, 2010, 139, e9-e10.	1.3	2
284	Postoperative Recurrence of Hepatocellular Carcinoma: The Importance of Distinguishing between Intrahepatic Metastasis and Multicentric Occurrence—Response. Clinical Cancer Research, 2019, 25, 5427-5427.	7.0	2
285	Malignant Mixed MÃ1⁄4llerian Tumor with Small Bowel Metastasis: A Case Report. Journal of the Korean Society of Magnetic Resonance in Medicine, 2012, 16, 257.	0.1	2
286	Necrotic lymphoma in a patient with post-transplantation lymphoproliferative disorder: ultrasonography and CT findings with pathologic correlation. Ultrasonography, 2015, 34, 148-152.	2.3	2
287	Validation of the Korean Liver Cancer Association-National Cancer Center 2018 Criteria for the Noninvasive Diagnosis of Hepatocellular Carcinoma Using Magnetic Resonance Imaging. Journal of Liver Cancer, 2020, 20, 120-127.	1.1	2
288	A lexicon for hepatocellular carcinoma surveillance ultrasonography: benign versus malignant lesions. Clinical and Molecular Hepatology, 2017, 23, 57-65.	8.9	2

#	Article	IF	CITATIONS
289	Portal venous perfusion steal causing graft dysfunction after orthotopic liver transplantation: serial imaging findings in a successfully treated patient. Ultrasonography, 2016, 35, 78-82.	2.3	2
290	Noninvasive Biomarker for Predicting Treatment Response to Concurrent Chemoradiotherapy in Patients with Hepatocellular Carcinoma. Investigative Magnetic Resonance Imaging, 2019, 23, 351.	0.4	2
291	Human Organic Anion Transporting Polypeptide 1B3 Applied as an MRI-Based Reporter Gene. Korean Journal of Radiology, 2020, 21, 726.	3.4	2
292	Virtual Colonoscopy with Electron Beam CT: Correlation with Barium Enema, Colonoscopy and Pathology. Journal of the Korean Radiological Society, 1998, 39, 123.	0.0	1
293	CT Findings of Perihepatic Tuberculous Abscess. Journal of the Korean Radiological Society, 1999, 41, 1161.	0.0	1
294	Hepatic Uptake of Gadoxetic Acid. Radiology, 2013, 267, 314-315.	7.3	1
295	Recent development of diagnostic imaging of hepatocellular carcinoma. Journal of the Korean Medical Association, 2013, 56, 948.	0.3	1
296	Letter to the editor. Abdominal Radiology, 2018, 43, 237-238.	2.1	1
297	Should LRâ€M and LRâ€TIV Remain Separate Categories in Llâ€RADS?. Hepatology, 2019, 69, 1842-1842.	7.3	1
298	Esophagographic Findings of Early Esophageal Cancer: Comparison with Pathologic Results. Journal of the Korean Radiological Society, 1998, 38, 869.	0.0	1
299	MR Evaluation of Rectal Carcinoma: Pelvic Phased-Array Coil versus Endorectal-Pelvic Phased-Array Coil. Journal of the Korean Radiological Society, 1998, 39, 733.	0.0	1
300	Non-contiguous Multi-organ Involvement of an Inflammatory Myofibroblastic Tumor: A Case Report. Journal of the Korean Radiological Society, 2007, 57, 265.	0.0	1
301	Primary Malignant Melanoma of the Esophagus: A Case Report. Journal of the Korean Radiological Society, 2007, 57, 37.	0.0	1
302	Preoperative Evaluation of Lower Rectal Cancer by Pelvic MR with and without Gel Filling. Journal of the Korean Society of Magnetic Resonance in Medicine, 2014, 18, 323.	0.1	1
303	Added Value of Arterial Enhancement Fraction Color Maps for the Characterization of Small Hepatic Low-Attenuating Lesions in Patients with Colorectal Cancer. PLoS ONE, 2015, 10, e0114819.	2.5	1
304	Optimal imaging criteria and modality to determine Milan criteria for the prediction of post-transplant HCC recurrence after locoregional treatment. European Radiology, 0, , .	4.5	1
305	CT colonography for postoperative surveillance after curative gastrectomy in patients with gastric cancer. Journal of Surgical Oncology, 2010, 102, 593-598.	1.7	0
306	An incidentally found complex cystic lesion in the liver. Liver International, 2011, 31, 970-970.	3.9	0

#	Article	IF	CITATIONS
307	Extraosseous Ewing's Sarcoma Presented as a Rectal Subepithelial Tumor: Radiological and Pathological Features. Investigative Magnetic Resonance Imaging, 2017, 21, 51.	0.4	0
308	A prospective study on the use of ultralow-dose computed tomography with iterative reconstruction for the follow-up of patients liver and renal abscess. PLoS ONE, 2021, 16, e0246532.	2.5	0
309	Gadoxetic Acid-Enhanced and Diffusion-Weighted Magnetic Resonance Imaging of Histologically Defined Early Hepatocellular Carcinoma. Korean Journal of Abdominal Radiology, 2021, 5, 17-31.	0.0	0
310	Granular Cell Tumor of the Presacral Space. American Journal of Roentgenology, 2000, 174, 1165-1166.	2.2	0
311	Detection of Hepatocellular Carcinoma: Comparison of Gadoxetic Acid-Enhanced MRI, Diffusion-Weighted Imaging, and Combined Interpretation at 3 T MRI. Journal of the Korean Society of Radiology, 2013, 69, 213.	0.2	0
312	Imaging of Nontraumatic Benign Splenic Lesions. Journal of the Korean Radiological Society, 1999, 40, 737.	0.0	0
313	Utility of Single Shot Fast Spin Echo Technique in Evaluating Pancreaticobiliary Diseases : T 2 - weighted Image and Magnetic Resonance Cholangiopancreatography. Journal of the Korean Radiological Society, 1999, 41, 515.	0.0	0
314	Anal Metastasis Originating from Colorectal Cancer: Report of Two Cases. Journal of the Korean Society of Radiology, 2016, 75, 501.	0.2	0
315	History of the Asian Society of Abdominal Radiology. Korean Journal of Radiology, 2020, 21, 5.	3.4	0
316	MRI Findings of Rectal Submucosal Tumors. Korean Journal of Radiology, 2011, 12, 496.	3.4	0
317	Diagnostic Image Feature and Performance of CT and Gadoxetic Acid Disodium-Enhanced MRI in Distinction of Combined Hepatocellular-Cholangiocarcinoma from Hepatocellular Carcinoma. Investigative Magnetic Resonance Imaging, 2021, 25, 313.	0.4	0